## EDGE ARTICLE

Check for updates

# Reductive electrophilic C–H alkylation of quinolines by a reusable iridium nanocatalyst†‡

Rong Xie, Wenhui Mao, Huanhuan Jia, Jialu Sun, Guangpeng Lu, Huanfeng Jiang [ID] and Min Zhang [ID] *

The incorporation of a coupling step into the reduction of unsaturated systems offers a desirable way for diverse synthesis of functional molecules, but it remains to date a challenge due to the difficulty in controlling the chemoselectivity. Herein, by developing a new heterogeneous iridium catalyst composed of Ir-species ($Ir^{\delta+}$) and N-doped $SiO_2/TiO_2$ support ($Ir/N\text{-}SiO_2/TiO_2$), we describe its application in reductive electrophilic mono and dialkylations of quinolines with various 2- or 4-functionalized aryl carbonyls or benzyl alcohols by utilizing renewable formic acid as the reductant. This catalytic transformation offers a practical platform for direct access to a vast range of alkyl THQs, proceeding with excellent step and atom-efficiency, good substrate scope and functional group tolerance, a reusable catalyst and abundantly available feedstocks, and generation of water and carbon dioxide as by-products. The work opens a door to further develop more useful organic transformations under heterogeneous reductive catalysis.

## Introduction

Over the past decade, hydrogen transfer-mediated coupling reactions have emerged as appealing tools in the construction of valuable products,[1] since there is no need for compressed $H_2$ gas and elaborate experimental setups. For instance, except for the well-established reductive amination,[2] the groups of Beller,[3] Kempe,[4] Kirchner,[5] Liu[6] and others[7] have achieved the alkylation of amines and the α-site of carbonyl compounds with the hydrogen-borrowing strategy. Bruneau and co-workers have realized the β-alkylation of N-substituted cyclic amines.[8] Li *et al.* demonstrated amine syntheses from abundantly available phenols.[9] Recently, our group reported a direct reductive quinolyl β-C–H alkylation with aldehydes.[10] In this process the heterogeneous Co-catalyst (CoOx/MSCC) effects the slow catalytic transfer hydrogenation (CTH) of the quinolines, thus favoring the coupling process (Scheme 1a; MSCC = multi-spherical cavity carbon). Despite these advances, the concept of merging the reduction of N-heteroarenes with a coupling step still encounters significant challenges, and one of the most important factors is that the N-heteroarenes tend to undergo multiple hydrogenations to form non-coupling cyclic amines.

Tetrahydroquinolines (THQs) constitute a class of significantly important N-heterocycles, and they frequently occur in bioactive natural products, and are widely utilized as versatile building blocks for the preparation of numerous fine chemicals, pharmaceuticals, agrochemicals, and functional materials.[11] Although the reduction of quinolines offers a useful way to directly access THQs,[12] its synthetic diversity is easily restricted due to the limited availability of quinolines. Motivated by the quinolyl[10] (Scheme 1a) and indolyl β-C–H alkylation[13] and the excellent CTH capability of iridium,[14] we initially envisioned a synthesis of alkyl THQs 3 *via* reductive Friedel–Crafts

*Key Lab of Functional Molecular Engineering of Guangdong Province, School of Chemistry and Chemical Engineering, South China University of Technology, Guangzhou 510641, People's Republic of China. E-mail: minzhang@scut.edu.cn*

**Scheme 1** Reductive alkylation of quinolines.

alkylation of 8-methylquinoline **1a** with different aryl carbonyls **2** (Scheme 1b). However, by utilizing renewable formic acid as a preferred reductant,[15] the reaction with different iridium complexes only generated alkyl benzenes **2″** and *N*-alkyl THQs **3′**, deriving from the hydrodeoxygenation of **2′** and reductive amination of THQ **1a′** and **2**, respectively. So, to achieve a selective synthesis of THQ **3**, at least two challenging issues have to be addressed: (1) the *in situ* formed intermediates should favor the electrophilic coupling process, rather than the formation of by-products **2″** and **3′**. (2) It is preferable to develop a compatible and reusable Ir-catalyst due to the high cost of noble metal.

Regarding the above challenging issues, we believe that the development of a suitable supported Ir-catalyst and application of *ortho* and *para* effects of functional groups might offer a solution for a desired synthetic purpose. As shown in Scheme 1c, the introduction of a –OH or –NH$_2$ group *ortho* or *para* to the carbonyl group of reactant **2** is able to afford more stable resonance form **A** or **B** of benzyl carbocation, deriving from CTH of **2** and acid-assisted dehydration of alcohol **2′**, which is beneficial to the conjugate addition of THQ **1′** (see **C** or **D**) to afford product **3**.

It is important to note that support dopants drastically affect the physicochemical properties of resulting supported catalysts including morphology, basicity and electrical conductivity.[16] Moreover, introduction of two or more dopants may exhibit synergistic effects on catalytic performace.[17] Attracted by these characteristics and the capability of silica for adjusting the micropore size of the supporting materials,[18] we report herein the preparation and characterization of a new N-doped SiO$_2$/TiO$_2$-supported iridium nanocatalyst, and describe, for the first time, its application in reductive electrophilic alkylation of quinolines, which offers a platform to directly access a wide range of alkyl THQs from abundantly available quinolines and aryl carbonyls or benzyl alcohols.

Typically, the iridium heterogeneous catalyst was prepared through the following procedure: a mixture of IrCl$_3$·3H$_2$O and 1,10-phenanthroline in 1 : 3 molar ratio in EtOH was initially refluxed at 80 °C for 1 hour to form the coordinated Phen–Ir complex. Then, the silica was introduced by *in situ* hydrolysis of Si(OC$_2$H$_5$)$_4$ (TEOS) with aqueous ammonia. After that, titanium dioxide powder (TiO$_2$ P25) was added and the mixture was stirred at 80 °C for 4 h. The resulting composites were pyrolyzed under Ar flow at 500 °C for 3 h after removing the solution, which afforded the supported iridium material Ir/N-SiO$_2$/TiO$_2$ (see the ESI‡ for details).

First, X-ray diffraction (XRD) was employed to test the constituents of the obtained iridium material. Except for the characteristic peaks of titanium dioxide (PDF no. 21-1276 and PDF no. 71-1166) and silicon dioxide (PDF no. 86-1563), no other significant peaks corresponding to the iridium species are found in the XRD pattern of Ir/N-SiO$_2$/TiO$_2$ (Fig. S1 in the ESI‡), suggesting that iridium species consist of a well-dispersed amorphous phase. The N$_2$ adsorption–desorption experiment shows a typical IV isotherm, which indicates the existence of mesoporous structure (Fig. S2 in ESI‡). Further, the BET specific surface area is detected as 110.06 m$^2$ g$^{-1}$, and the
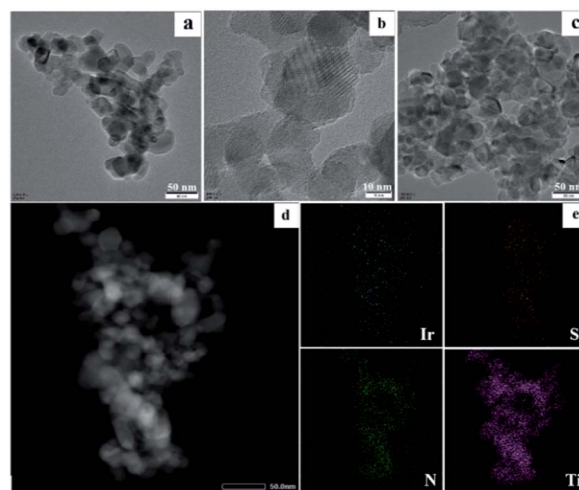


**Fig. 1** (a and b) TEM, HRTEM images of Ir/N-SiO$_2$/TiO$_2$. (c) TEM images of the reused Ir/N-SiO$_2$/TiO$_2$ after ten runs. (d) STEM images of Ir/N-Si−TiO$_2$ and (e) the corresponding elemental mapping of Ir, Si, N, Ti.

corresponding pore size is approximately concentrated around 20 nm (Fig. S2 in ESI‡), which further supports the mesoporous structure of the iridium-based material.

Then, the morphology of the Ir/N-SiO$_2$/TiO$_2$ material was analyzed by TEM, HRTEM, and EDS techniques. The TEM and HRTEM images (Fig. 1a and b) do not show individual Ir clusters, illustrating that the iridium species are uniformly dispersed, which are in good accordance with the XRD results. In addition, the element mapping images (Fig. 1e and S3‡) also reveal that the elements of Ir, Ti, Si, N, C and O are highly overlapped and interconnected with each other, and the iridium species are embedded on the doped support. The initial coordination between the 1,10-phenanthroline (Phen) and iridium constitutes the key to prevent the iridium from agglomeration during pyrolysis process.

To further analyze the surface chemistry of the prepared iridium material, X-ray photoelectron spectroscopy (XPS) characterization was implemented. A range of elements corresponding to Ir, N, Si, C, O and Ti on the sample surface were detected as 0.56%, 1.68%, 11.4%, 30.93%, 43.48% and 11.95%, respectively, which are in accordance with the elemental mapping results (Fig. S3 in the ESI‡). In comparison with the
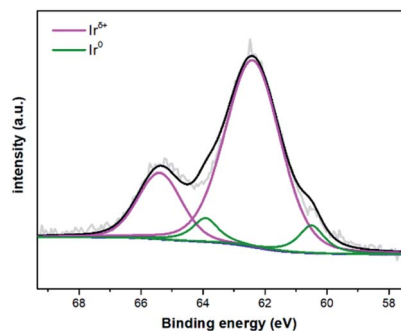


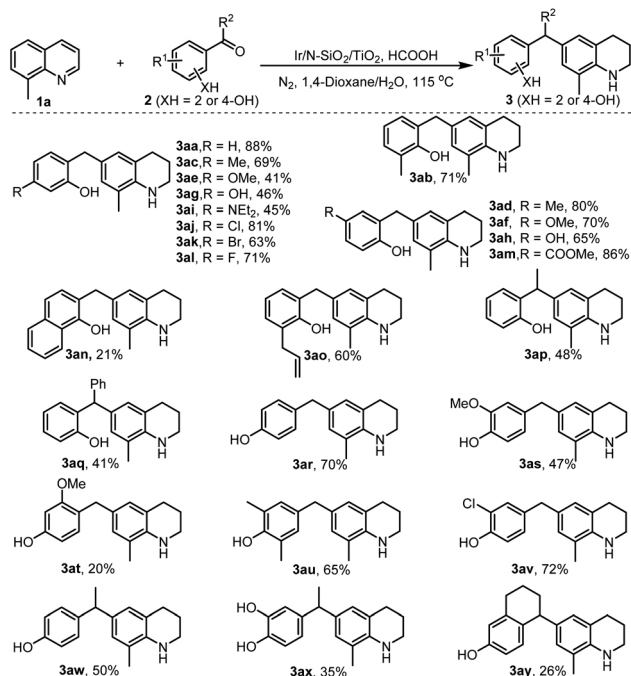**Fig. 2** Ir 4f XPS spectra of Ir/N-SiO$_2$/TiO$_2$.

initial N : Ir ratio of the starting materials (6 : 1), a 3 : 1 ratio of the N and Ir on the resulting catalyst surface indicates that three N-atoms are bound to one Ir-atom, whereas the unbound N-atoms are sparsely distributed on the material surface and could not be accurately detected by XPS.[19] The N 1s XPS spectrum (Fig. S4b in the ESI‡) discloses almost one peak, corresponding to pyridinic N (399.9 eV),[20] which derives from the Phen-ligand coordinated to iridium. The spectrum of Ir 4f (Fig. 2) shows four peaks, two typical characteristic peaks located at 62.4 eV and 65.4 eV are assigned to $Ir^{\delta+}$ species,[21] while the binding energy of 60.5 eV and 63.9 eV belong to the peaks of metallic Ir.[21b,22]

To investigate the catalytic performance of the developed nanomaterial, we chose the reaction of 8-methylquinoline **1a** and salicylaldehyde **2a** as a model system. After a systematic investigation of various reaction parameters, an optimal isolated yield of product **3aa** was obtained when the reaction in mixed solution $H_2O$/dioxane (8/1) was performed at 115 °C for 24 h in the presence of 0.65 mol% of catalyst using HCOOH as the reductant (standard condition, see Table S1 in ESI‡).
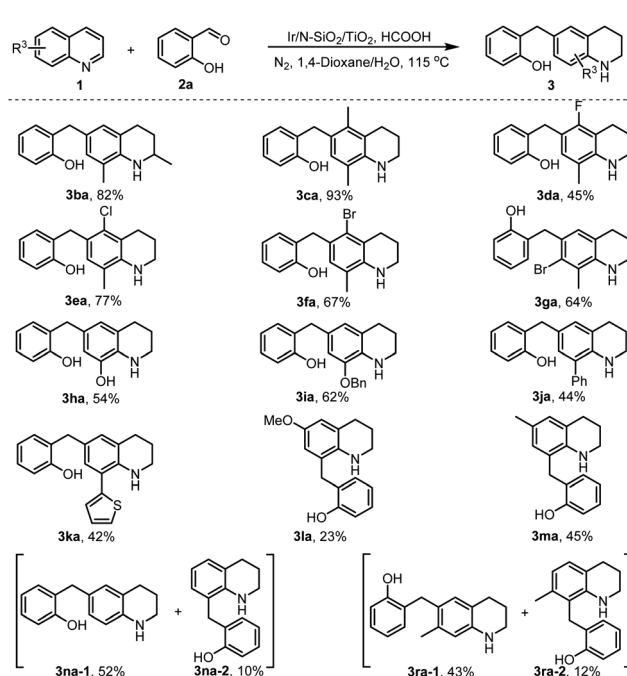
With the optimal reaction conditions available, we then set out to explore the universality of the developed chemistry. Initially, we tested the reductive electrophilic alkylation of quinoline with salicylaldehyde, but the reaction generated a mixture of $C_6$- and $C_8$-alkyalted THQs as well as $C_{6,8}$-dialkylated THQ in 49, 8, and 14% yields, respectively. So, we employed 8-methylquinoline **1a** to react with different kinds of salicylaldehydes (**2a–2o**, see Scheme S1 for their structures in ESI‡). As shown in Scheme 2, all the reactions proceeded smoothly and furnished $C_6$-alkylated THQs in reasonable to excellent isolated yields (**3aa–3ao**). Various functional groups (–Me, –OMe, –OH, –$NEt_2$, –$CO_2Me$, allylic, halogens) were well

tolerated in the transformation. The retention of these functionalities offers the potential for post-functionalization of the obtained alkyl THQs. Noteworthily, reactants **2** bearing electron-withdrawing groups (**3aj–3am**) afforded much higher product yields than those with electron-donating ones (**3ae**, **3ag**, and **3ai**). This phenomenon is attributed to electron-withdrawing groups favoring the formation of more reactive electrophilic intermediates (see Scheme 1c). In addition to salicylaldehydes and *o*-hydroxyaryl ketones (**2p** and **2q**), 4-hydroxyaryl aldehydes (**2r–2v**) and 4-hydroxyaryl ketones (**2w–2y**) were also applicable for the reaction, delivering the desired products in reasonable to good yields (**3ap–3ay**).

Subsequently, we turned our attention to the variation of substituted quinolines **1** by employing salicylaldehyde **2a** as a benchmark substrate (Scheme 3). First, various $C_8$-substituted quinolines (**1b–1k**, see Scheme S1 for their structures in ESI‡) were tested. All the reactions smoothly afforded the $C_6$-alkylated tetrahydroquinolines in moderate to excellent isolated yields (**3ba–3ka**). It was found that quinolines bearing an electron-donating group (**3ba–3ca** and **3ha–3ia**) afforded the desired products in higher yields than those having an electron-withdrawing group (**3da**, and **3ja–3ka**), which is assigned to the *in situ* formed THQs arising from catalytic transfer hydrogenation (CTH) of the electron-rich quinolines favoring the electrophilic coupling process (Scheme 1c). Gratifyingly, the reactions of $C_6$-substituted quinolines (**1l** and **1m**) were able to produce the $C_8$-alkylated THQs, albeit the product yields were somewhat low (**3la** and **3ma**). In addition to $C_6$ and $C_8$-substituted quinolines, $C_6$ and $C_8$ non-substituted quinolines (**1n** and **1r**) were also amenable to the transformation. Interestingly, they resulted in two easily separable regioisomers, and the 6-alkylated and 8-alkylated THQs were afforded as the major



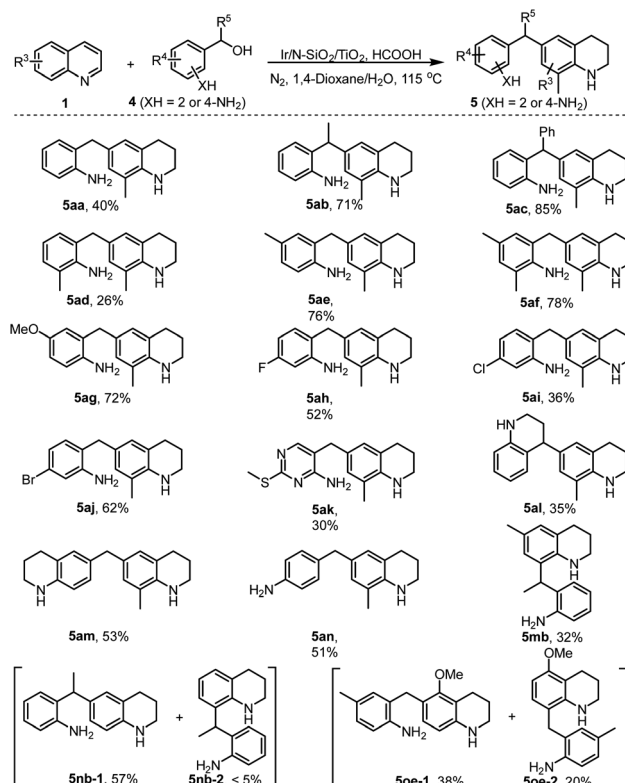**Scheme 2** Variation of 2- and 4-hydroxyaryl ketones.



**Scheme 3** Monoalkylation of various quinolines.

and minor products, respectively (**3na-1** and **3na-2**, **3ra-1** and **3ra-2**). These examples show that the developed chemistry enables to afford $C_6$- and $C_8$-nonsubstituted alkyl THQs. Noteworthily, all the halogenated reactants (**3aj–3al** and **3da–3ga**) in Schemes 2 and 3 did not undergo hydrodehalogenation, a side reaction occurring frequently in homogeneous reductive catalysis, showing that the developed heterogeneous catalyst merits good chemoselectivity in the current transformation.

Encouraged by the $C_6$ and $C_8$-alkylations described in Schemes 2 and 3, we then tested the dialkylation of quinolyl $C_6$ and $C_8$-sites. Thus, various $C_6$ and $C_8$ non-substituted quinolines (**1n–1s**) were employed to couple with sufficient salicylaldehyde (**2a**). As shown in Scheme 4, all the reactions smoothly generated the desired dialkylated products (**3**) in moderate to excellent yields upon isolation (**3naa–3saa**). Interestingly, except for the quinolines, *N*-alkyl anilines were also applicable for the catalytic transformation. For instance, *N,N*-dimethylaniline (**1t**) and *N*-methylaniline (**1u**) directly coupled with salicylaldehyde **2a** to afford the $C_2$ and $C_4$-dialkylated products (**3taa** and **3uaa**). These two examples demonstrate the potential of the developed chemistry in further synthesis of functionalized anilines, a class of synthetically useful compounds applied for numerous purposes.

Further, in consideration of the easy occurrence of cross-condensation between two molecules of 2-aminoaryl carbonyls, we therefore turned our attention to the transformation of 2-aminobenzyl alcohols **4** including one 2-aminoheteroaryl example (**4k**) with quinoline **1a**. Gratifyingly, all the reactions efficiently afforded the desired 6-(2-aminobenzyl) THQs in reasonable to high isolated yields (Scheme 5, **5aa–5ak**). Noteworthily, α-phenyl substituted alcohol **4c** afforded relatively higher product yield (**5ac**) than other 2-aminobenzyl alcohols (**5aa** and **5ad–5ak**), which is attributed to such a substrate (**4c**) favoring the formation of more stable electrophilic intermediate (Scheme 1c). Interestingly, 1,2,3,4-tetrahydroquinolin-4-ol **4l** and 6-hydroxymethyl THQ **4m**
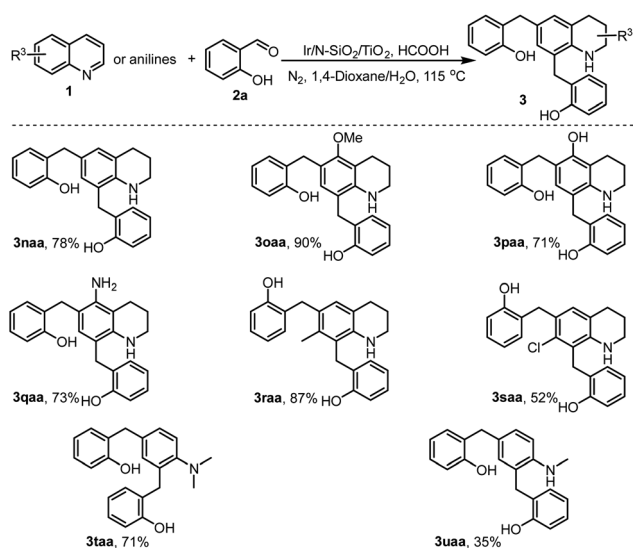


**Scheme 5** The application of 2- or 4-aminobenzyl alcohols.

effectively coupled with quinoline **1a**, affording the products featuring two tetrahydroquinolyl motifs in moderate yields (**5al** and **5am**). 4-Hydroxymethyl aniline **4n** also underwent efficient reductive alkylation to afford product **5an** in 51% yield. Similar to the result described in Scheme 3, the reaction of $C_6$-substituted quinoline **1m** and alcohol **4b** produced the $C_8$-alkylated THQ **5mb** in 32% yield. The $C_6$ and $C_8$ non-substituted quinolines (**1n** and **1o**) smoothly coupled with amino alcohols (**4b** and **4e**) to give two sets of separable regioisomers in reasonable yields (**5nb-1** and **5nb-2**, **5oe-1** and **5oe-2**). It is important to note that all products in Scheme 5 possess two amino groups, which could serve as a class of valuable compounds for the preparation of functional polyamides.

To examine the stability of the newly developed heterogeneous catalyst, we performed recycling experiments with the model reaction. As shown in Fig. 3, the catalytic activity maintained very well even after ten consecutive runs, albeit with a slight decline of product yields, which is assigned to the aggregation of some smaller nanoparticles and the mechanical abrasion during the reaction. Furthermore, the XRD spectrum, TEM images and Ir 4f XPS spectra (Fig. 1c, S1 and S4c in ESI‡) of the used $Ir/N-SiO_2/TiO_2$ material after 10 runs clearly demonstrate that its morphology is well retained, thus revealing that the catalyst has excellent stability.
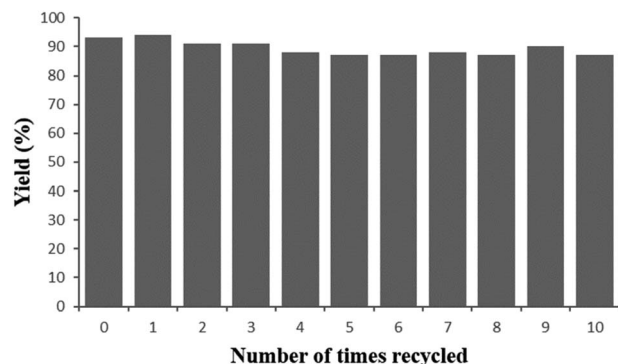
To gain mechanistic insights into the reaction, several control experiments were performed. First, the model reaction was interrupted after 1 h, which resulted in product **3aa**, THQ **1a′** and 2-hydroxybenzyl alcohol **2a′** in 2%, 80%, and 5% yields,
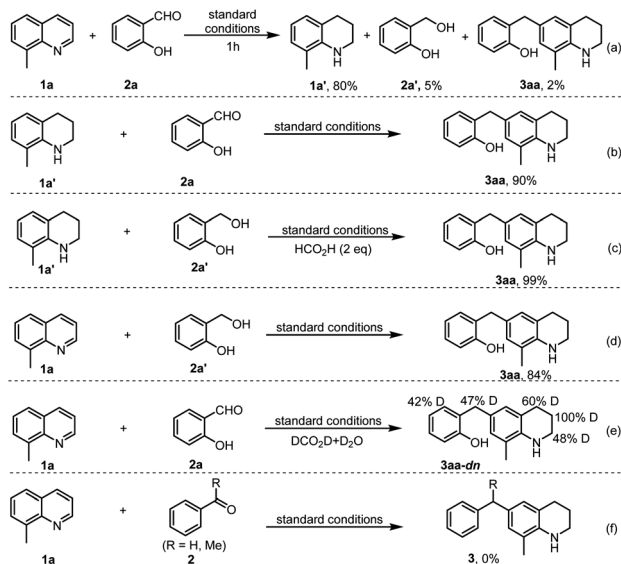


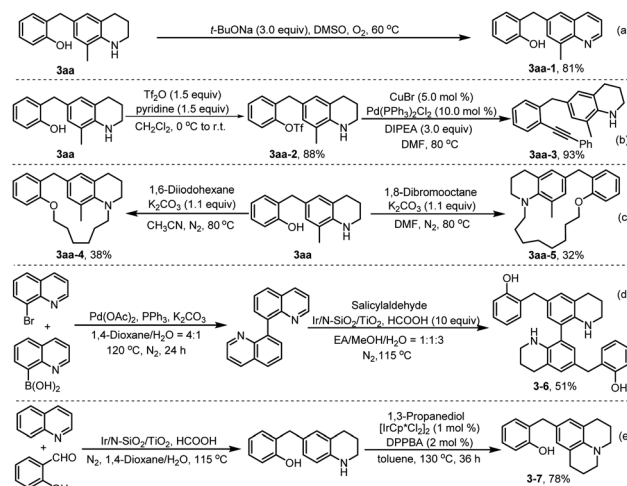**Scheme 4** Dialkylation of various quinolines.

**Fig. 3** Reusability of the Ir/N–SiO$_2$/TiO$_2$ catalyst.

respectively (Scheme 6a). Under the standard conditions, the reaction of THQ **1a′** with salicylaldehyde **2a** or 2-(hydroxymethyl)phenol **2a′**, or the coupling of quinoline **1a** with **2a′** all generated product **3aa** in excellent yields (Scheme 6b–d), which support that compounds **1a′** and **2a′** are key reaction intermediates. Further, by replacing aqueous HCOOH with DCOOD in D$_2$O, the reaction of 8-methylquinoline **1a** and salicylaldehyde **2a** generated product **3aa**-*dn* with different D-ratios at the α, β, γ and benzylic sites (Scheme 6e), indicating that HCO$_2$H serves as the hydrogen donor, and there exists a hydrogenation of reactant **2a** and a tautomerization during the formation of reactive electrophilic intermediates. Noteworthy, benzaldehyde or acetophenone failed to couple with 8-methylquinoline (**1a**) to give target products **3** (Scheme 6f). Therefore, all these results are in good agreement with the proposed reaction pathway in Scheme 1c. In addition, the poisoning experiment by addition of KSCN to the model reaction led to loss of catalyst activity in the formation of the target product **3aa**,[23] which reveals that the Ir$^{\delta+}$ species serve as the catalytically active sites.



**Scheme 6** Control experiments.



**Scheme 7** Synthetic applications.

To explore the utility of the developed chemistry, further transformations of product **3aa** were conducted. As shown in Scheme 7, a mixture of compound **3aa** and *t*-BuONa in DMSO was stirred at 60 °C under O$_2$ atmosphere for 6 h, which resulted in dehydroaromatization product **3aa-1** in 81% yield (Scheme 7a).[24] In addition, treatment of **3aa** with Tf$_2$O and pyridine in dichloromethane solution at room temperature for 6 h initially produced a trifluoromethanesulfonylated product **3aa-2** in 88% yield,[25] which then underwent palladium-catalysed Sonogashira cross-coupling with phenylacetylene, to afford product **3aa-3** in 93% yield (Scheme 7b). The coupling of compound **3aa** with dihaloalkanes produced medium-sized ring products (**3aa-4** and **3aa-5**) in reasonable yields, which shows the potential of the obtained compounds in further construction of different cyclic products by mediating the chain-length of difunctionalized agents (Scheme 7c). Further, the synthetic method was successfully applied to reductive dialkylation of bisquinoline, affording the bistetrahydroquinoline **3–6** in 51% yield (Scheme 7d), a promising candidate for the development of optoelectronic materials and nitrogen-containing ligands.[26] Finally, product **3–7**, an analogue of therapeutical molecule used for the treatment of tauopathies,[27] was prepared in high yield by hydrogen transfer-mediated annulation of C$_6$-alkylated THQ **3aa** with 1,3-propanediol (Scheme 7e).[28]

## Conclusions

A heterogeneous nanocatalyst composed of iridium and nitrogen-doped SiO$_2$/TiO$_2$ support (Ir/N-SiO$_2$/TiO$_2$) is successfully applied to reductive electrophilic alkylation of quinolines with salicylaldehydes, 4-hydroxyaryl ketones, and 2- or 4-aminobenzylic alcohols. The catalytic transformation proceeds with good substrate and functional group compatibility, uses reusable catalyst and abundantly available feedstocks, and generates water and carbon dioxide as by-products, which offers a practical platform for direct access to a vast range of carboalkylated tetrahydroquinolines, a class of significantly important compounds employed frequently for the discovery and

preparation of functional products. The strategy applying activity-tunable characteristic of supported heterogeneous catalysts in reductive coupling is anticipated to further develop more useful but challenging organic transformations.

## Data availability

The datasets supporting this article have been uploaded as part of the ESI.‡

## Author contributions

R. X. performed the experiments and the data analyses, and wrote the manuscript draft. M. Z. conceived the idea, revised the manuscript, and directed the project. W. M. provided some experimental assistance. H. J., J. S. and G. L. discussed and analysed the data of the catalyst. H. F. J. suggested the substrate scope and discussed the reaction mechanism.

## Conflicts of interest

There are no conflicts to declare.

## Acknowledgements

## Notes and references

1 (a) W. Y. Ai, R. Zhong, X. F. Liu and Q. Liu, *Chem. Rev.*, 2019, **119**, 2876–2953; (b) T. Irrgang and R. Kempe, *Chem. Rev.*, 2019, **119**, 2524–2549; (c) M. Holmes, L. A. Schwartz and M. J. Krische, *Chem. Rev.*, 2018, **118**, 6026–6052; (d) X. W. Chen, H. Zhao, C. L. Chen, H. F. Jiang and M. Zhang, *Angew. Chem., Int. Ed.*, 2017, **56**, 14232–14236.

2 Selected examples: (a) Y. Chen, Y. M. He, S. S. Zhang, T. T. Miao and Q. H. Fan, *Angew. Chem., Int. Ed.*, 2019, **58**, 3809–3813; (b) Y. Chen, Y. X. Pan, Y. M. He and Q. H. Fan, *Angew. Chem., Int. Ed.*, 2019, **58**, 16831–16834; (c) O. I. Afanasyev, E. Kuchuk, D. L. Usanov and D. Chusov, *Chem. Rev.*, 2019, **119**, 11857–11911.

3 (a) S. Elangovan, J. Neumann, J.-B. Sortais, K. Junge, C. Darcel and M. Beller, *Nat. Commun.*, 2016, **7**, 12641; (b) S. Elangovan, J.-B. Sortais, M. Beller and C. Darcel, *Angew. Chem., Int. Ed.*, 2015, **54**, 14483–14486.

4 (a) F. Kallmeier, R. Fertig, T. Irrgang and R. Kempe, *Angew. Chem., Int. Ed.*, 2020, **59**, 11789–11793; (b) G. Y. Zhang, T. Irrgang, T. Dietel, F. Kallmeier and R. Kempe, *Angew. Chem., Int. Ed.*, 2018, **57**, 9131–9135; (c) N. Deibl and R. Kempe, *J. Am. Chem. Soc.*, 2016, **138**, 10786–10789; (d) S. Roesler, M. Ertl, T. Irrgang and R. Kempe, *Angew. Chem., Int. Ed.*, 2015, **54**, 15046–15050.

5 (a) M. Mastalir, B. Stoeger, E. Pittenauer, M. Puchberger, G. Allmaier and K. Kirchner, *Adv. Synth. Catal.*, 2016, **358**, 3824–3831; (b) M. Mastalir, G. Tomsu, E. Pittenauer, G. Allmaier and K. Kirchner, *Org. Lett.*, 2016, **18**, 3462–3465.

6 (a) Y. Wang, Z. Shao, K. Zhang and Q. Liu, *Angew. Chem., Int. Ed.*, 2018, **57**, 15143–15147; (b) S. Fu, Z. Shao, Y. Wang and Q. Liu, *J. Am. Chem. Soc.*, 2017, **139**, 11941–11948.

7 Selected examples: (a) T. Liu, L. Wang, K. Wu and Z. Yu, *ACS Catal.*, 2018, **8**, 7201–7207; (b) M. Vellakkaran, K. Singh and D. Banerjee, *ACS Catal.*, 2017, 7, 8152–8158; (c) F. Huang, Z. Liu and Z. Yu, *Angew. Chem., Int. Ed.*, 2016, **55**, 862–875; (d) Z. J. Xu, X. L. Yu, X. X. Sang and D. W. Wang, *Green Chem.*, 2018, **20**, 2571–2577; (e) D. Wang, K. Zhao, C. Xu, H. Miao and Y. Ding, *ACS Catal.*, 2014, **4**, 3910–3918.

8 (a) K. Yuan, F. Jiang, Z. Sahli, M. Achard, T. Roisnel and C. Bruneau, *Angew. Chem., Int. Ed.*, 2012, **51**, 8876–8880; (b) B. Sundararaju, M. Achard, G. V. M. Sharma and C. Bruneau, *J. Am. Chem. Soc.*, 2011, **133**, 10340–10343; (c) Z. Sahli, B. Sundararaju, M. Achard and C. Bruneau, *Green Chem.*, 2013, **15**, 775–779.

9 (a) Z. Qu, H. Zeng and C. Li, *Acc. Chem. Res.*, 2020, **53**, 2395–2413; (b) Z. Chen, H. Zeng, H. Gong, H. Wang and C.-J. Li, *Chem. Sci.*, 2015, **6**, 4174–4178; (c) Z. Chen, H. Zeng, S. A. Girard, F. Wang, N. Chen and C.-J. Li, *Angew. Chem., Int. Ed.*, 2015, **54**, 14487–14491.

10 F. Xie, R. Xie, J. X. Zhang, H. F. Jiang, L. Du and M. Zhang, *ACS Catal.*, 2017, **7**, 4780–4785.

11 (a) J. D. Scott and R. M. Williams, *Chem. Rev.*, 2002, **102**, 1669–1730; (b) R. Rahi, M. Fang, A. Ahmed and R. A. Sanchez-Delgado, *Dalton Trans.*, 2012, **41**, 14490–14497; (c) I. Muthukrishnan, V. Sridharan and J. C. Menendez, *Chem. Rev.*, 2019, **119**, 5057–5191.

12 (a) K. Murugesan, V. G. Chandrashekhar, C. Kreyenschulte, M. Beller and R. V. Jagadeesh, *Angew. Chem., Int. Ed.*, 2020, **59**, 17408–17412; (b) A. Vivancos, M. Beller and M. Albrecht, *ACS Catal.*, 2018, **8**, 17–21; (c) D. S. Wang, Q. A. Chen, S. M. Lu and Y. G. Zhou, *Chem. Rev.*, 2012, **112**, 2557–2590.

13 J. R. Cabrero-Antonino, R. Adam, K. Junge and M. Beller, *Chem. Sci.*, 2017, **8**, 6439–6450.

14 (a) S. Ott, *Science*, 2011, **333**, 1714–1715; (b) R. Nie, Y. Tao, Y. Nie, T. Lu, J. Wang, Y. Zhang, X. Lu and C. C. Xu, *ACS Catal.*, 2021, **11**, 1071–1095; (c) R. Xie, G.-P. Lu, H.-F. Jiang and M. Zhang, *J. Catal.*, 2020, **383**, 239–243; (d) R. Xie, F. Xie, C.-J. Zhou, H.-F. Jiang and M. Zhang, *J. Catal.*, 2019, **377**, 449–454.

15 (a) K. Gong, F. Du, Z. Xia, M. Durstock and L. Dai, *Science*, 2009, **323**, 760–764; (b) S. Lu, C. Li, H. Li, Y. Zhao, Y. Gong, L. Niu, X. Liu and T. Wang, *Appl. Surf. Sci.*, 2017, **392**, 966–974; (c) Q. Zhou, W. Ju, X. Su, Y. Yong, X. Li, Z. Fu and C. Wang, *RSC Adv.*, 2017, **7**, 43521–43530; (d) J. Wang, Z. Xu, Y. Gong, C. Han, H. Li and Y. Wang, *ChemCatChem*, 2014, **6**, 1204–1209.

16 (a) K. Gong, F. Du, Z. Xia, M. Durstock and L. Dai, *Science*, 2009, **323**, 760–764; (b) S. Lu, C. Li, H. Li, Y. Zhao, Y. Gong, L. Niu, X. Liu and T. Wang, *Appl. Surf. Sci.*, 2017, **392**, 966–

974; (c) Q. Zhou, W. Ju, X. Su, Y. Yong, X. Li, Z. Fu and C. Wang, *RSC Adv.*, 2017, **7**, 43521–43530.

17 (a) Z. Li, Y. Li, Y. Wang and X. Wang, *Can. J. Phys.*, 2016, **94**, 929–932; (b) J. A. Talla and A. A. Ghozlan, *Chin. J. Phys.*, 2018, **56**, 740–746.

18 (a) S. M. Sachau, M. Zaheer, A. Lale, M. Friedrich, C. E. Denner, U. B. Demirci, S. Bernard, G. Motz and R. Kempe, *Chem. –Eur. J.*, 2016, **22**, 15508–15512; (b) J. Yoo, J.-I. Kim, H.-J. Cho, S.-S. Choo, S.-I. Kim, K. Lee, W. H. Shin, H.-S. Kim and J. W. Roh, *Phys. Soc.*, 2018, **72**, 775–779; (c) H. L. Jia, B. G. Ren, M. Li, X. J. Liu, J. X. Wu and X. Tan, *Solid State Commun.*, 2018, **277**, 45–49.

19 F. A. Westerhaus, R. V. Jagadeesh, G. Wienhofer, M. M. Pohl, J. Radnik, A. E. Surkus, J. Rabeah, K. Junge, H. Junge, M. Nielsen, A. Bruckner and M. Beller, *Nat. Chem.*, 2013, **5**, 537–543.

20 Y. Cao, S. Mao, M. Li, Y. Chen and Y. Wang, *ACS Catal.*, 2017, **7**, 8090–8112.

21 (a) Y. Xing, Y. Yang, D. Li, M. Luo, N. Chen, Y. Ye, J. Qian, L. Li, D. Yang, F. Wu, R. Chen and S. Guo, *Adv. Mater.*, 2018, **30**, 1803124; (b) W. Cao, L. Lin, H. Qi, Q. He, Z. Wu, A. Wang, W. Luo and T. Zhang, *J. Catal.*, 2019, **373**, 161–172.

22 (a) S. J. Freakley, J. Ruiz-Esquius and D. J. Morgan, *Surf. Interface Anal.*, 2017, **49**, 794–799; (b) M. Scohy, S. Abbou, V. Martin, B. Gilles, E. Sibert, L. Dubau and F. Maillard, *ACS Catal.*, 2019, **9**, 9859–9869; (c) R. Jin, M. Peng, A. Li, Y. Deng, Z. Jia, F. Huang, Y. Ling, F. Yang, H. Fu, J. Xie, X. Han, D. Xiao, Z. Jiang, H. Liu and D. Ma, *J. Am. Chem.*

*Soc.*, 2019, **141**, 18921–18925; (d) Y. Zhang, Z. Zhang, X. Yang, R. Wang, H. Duan, Z. Shen, L. Li, Y. Su, R. Yang, Y. Zhang, X. Su, Y. Huang and T. Zhang, *Green Chem.*, 2020, **22**, 6855–6861.

23 (a) C. Tang, A. E. Surkus, F. Chen, M. M. Pohl, G. Agostini, M. Schneider, H. Junge and M. Beller, *Angew.Chem. Int. Ed.*, 2017, **56**, 16616–16620; (b) Z. Ma, T. Song, Y. Yuan and Y. Yang, *Chem. Sci.*, 2019, **10**, 10283–10289; (c) H. Luo, L. Wang, S. Shang, G. Li, Y. Lv, S. Gao and W. Dai, *Angew.Chem. Int. Ed.*, 2020, **59**, 19268–19274.

24 R. Yang, S. Yue, W. Tan, Y. Xie and H. Cai, *J. Org. Chem.*, 2020, **85**, 7501–7509.

25 L. Cao, H. Zhao, Z. D. Tan, R. Q. Guan, H. F. Jiang and M. Zhang, *Org. Lett.*, 2020, **22**, 4781–4785.

26 (a) C. Wang, D. M. Flanigan, L. N. Zakharov and P. R. Blakemore, *Org. Lett.*, 2011, **13**, 4024–4027; (b) T. P. Loh and J. Xiao, *US Pat.*, 2012088916A1, 2012.

27 (a) S. Clunas, J. M. D. Strory, J. E. Rickard, D. Horsley, C. R. Harrington and C. M. Wischik, *GB Pat.*, WO2010067078A2, 2010; (b) M. A. Delong, K. A. Biedermann, D. L. Bissett, A. S. Boyer, S. L. Cohen and C. E. Snider, *US Pat.*, WO2004037213A2, 2004; (c) G. Q. Xu, Z. T. Feng, J. T. Xu, Z. Y. Wang, Y. Qin and P. F. Xu, *Chem. –Eur. J.*, 2018, **24**, 13778–13782.

28 A. Labed, F. Jiang, I. Labed, A. Lator, M. Peters, M. Achard, A. Kabouche, Z. Kabouche, G. V. M. Sharma and C. Bruneau, *ChemCatChem*, 2015, **7**, 1090–1096.